pISSN 1229-845X, eISSN 1976-555X
J. Vet. Sci. (2014), **15**(1), 149-155
http://dx.doi.org/10.4142/jvs.2014.15.1.149
Received: 16 Jul. 2012, Revised: 7 Nov. 2012, Accepted: 24 Dec. 2012

JOURNAL OF
Veterinary
Science

Original Article

Echocardiographic assessment of coronary artery flow in normal canines and model dogs with myocardial infarction

Nohwon Park, Jaehwan Kim, Miyoung Lee, Soyun Lee, Sunhye Song, Seungjun Lee, Soyoung Kim, Yangwoo Park, Kidong Eom*

Department of Veterinary Radiology and Diagnostic Imaging, College of Veterinary Medicine, Konkuk University, Seoul 143-701, Korea

This study was conducted to evaluate the usefulness of coronary arterial profiles from normal dogs (11 animals) and canines (six dogs) with experimental myocardial infarction (MI) induced by ligation of the left coronary artery (LCA). Blood velocity of the LCA and right coronary artery (RCA) were evaluated following transthoracic pulsed-wave Doppler echocardiography. The LCA was observed as an infundibular shape, located adjacent to the sinus of Valsalva. The RCA appeared as a tubular structure located 12 o'clock relative to the aorta. In normal dogs, the LCA and RCA mean peak diastolic velocities were 20.84 ± 3.24 and 19.47 ± 2.67 cm/sec, respectively. The LCA and RCA mean diastolic deceleration times were 0.91 ± 0.14 sec and 1.13 ± 0.20 sec, respectively. In dogs with MI, the LCA had significantly ($p < 0.01$) lower peak velocities (14.82 ± 1.61 cm/sec) than the RCA (31.61 ± 2.34 cm/sec). The RCA had a significantly ($p < 0.01$) rapid diastolic deceleration time (0.71 ± 0.06 sec) than that found in the LCA (1.02 ± 0.22 sec) of MI dogs. In conclusion, these profiles may serve as a differential factor for evaluating cardiomyopathy in dogs.

Keywords: coronary artery, dog, echocardiography, myocardial infarction, peak diastolic velocity

Introduction

Coronary flow velocity and coronary flow reserve measurements provide useful clinical and physiological information in humans [17]. Until recently, coronary artery disease was conventionally evaluated by assessing regional and global left ventricular function with the patient at rest and under stress [34]. Imaging techniques that enable direct visualization of the coronary arteries include Doppler guidewire [1], computed tomographic angiography [22,24,25], transesophageal [33] or intracardiac echocardiography [30], and magnetic resonance angiography [3,20]. These techniques are invasive and expensive [34], and their use in veterinary medicine is therefore limited.

The measurement of coronary flow velocity using transthoracic Doppler echocardiography was first described in human medicine in 1987 [34]. Since then, visualization of the coronary arteries and blood flow assessment using transthoracic echocardiography has improved owing to technological advances in ultrasonography with the aid of digital imaging using a high-frequency transducer [34]. Transthoracic echocardiography is a noninvasive, inexpensive, and reproducible technique for monitoring coronary arterial flow [17]. However, transthoracic echocardiography for evaluating coronary flow velocities has not been utilized in veterinary medicine to the best of our knowledge. The purpose of this study was to evaluate the ability of echocardiographic techniques to measure peak diastolic velocity in the coronary arteries of clinically healthy beagles. In addition, coronary artery flow in normal dogs was compared to that observed in a canine model of myocardial infarction (MI).

Materials and Methods

The Institutional Animal Care and Use Committee of Konkuk University (Korea) approved the study protocol (IACUC No. KU11059). In total, 17 beagles were included in the investigation: 11 were in the control group (seven males and four females) and were six included in the MI group (four males and two females). All dogs were purchased from Beijing Marshall Biotechnology (China).

*Corresponding author: Tel: +82-2-450-4165; Fax: +82-2-444-4396; E-mail: eomkd@konkuk.ac.kr

The median weight of the dogs was 9.43 kg (range: 8.5～10.5 kg) and the median age was 22.8 months (range: 15～28 months). Following clinical and laboratory examinations, all the dogs were found to be in good health. Results from the physical examination, hematology, serology, electrocardiography, radiography, and echocardiography were all normal. The dogs were also negative for heartworm infections according to the *Dirofilaria immitis* antigen test and microscopy evaluation of blood samples.

Six canines in the MI group had previously undergone surgical ligation of the left anterior descending (LAD) artery below the first diagonal branch. Medetomidine (0.02 mg/kg, intravenously, Domitor; Oricon Corporation Animal Health, Finland) was used for sedation 20 min before surgery and propofol (5 mg/kg, intravenously, Anepol; Hana Pharma, Korea) was administered to induce anesthesia. The dogs were intubated with an endotracheal tube and anesthesia was maintained with isoflorane (1.5～2% in 100% oxygen through the endotracheal tube, Foran; JW Pharmaceutical, Korea).

The dogs were placed in a right lateral recumbent position and left thoracotomy was performed at the level of the 5th intercostal space. After thoracotomy, the pericardial sac was incised and the exposed paraconal branch of the left coronary artery was permanently ligated using non-absorbable suture material (Prolene; Johnson & Johnson Medical, USA) below the first diagonal branch to induce MI. Lidocaine (Daehan Lidocaine HCl 2%; Daehan Pharma, Korea) was injected as a 2 mg/kg intravenous bolus before coronary artery ligation was performed. This compound was then administrated as an intravenous infusion at a constant rate of 0.05 mg/kg/min during the rest of the surgical procedure to prevent ventricular tachycardia. MI was confirmed by immediate ST segment elevation on electrocardiography and a color change of the myocardium to blue. After coronary artery ligation, the pericardium and thoracic wall was closed with absorbable suture material (Maxon; Covidien, Ireland). Tramadol (5 mg/kg, intravenously, Tridol amp.; Yuhan Corporation, Korea) and cephradine (30 mg/kg, intravenously, Cefradine; Sinil Pharm, Korea) were administrated for pain control and to prevent infection, respectively.

Echocardiography was performed using ultrasound (Prosound alpha7; Hitachi Aloka Medical, Japan) and a 3～8-MHz broad-frequency sector transducer a month after MI induction while the dogs were conscious. Ultrasonographic scanning was performed using 6.15 MHz color Doppler flow imaging. To obtain images of optimal quality, the velocity range and gain setting were adjusted accordingly. To make a complete assessment, both the left coronary artery (LCA) and right coronary artery (RCA) were examined in this study. To evaluate the LCA, all the dogs were examined while in a right lateral recumbent position and an acoustic window was created in the fourth or fifth intercostal spaces. If images of the aorta were obtained in the right parasternal long-axis left ventricular outflow view, then the area anterior to the left ventricular outflow tract and left interventricular sulcus were examined using 2D imaging in combination with color flow mapping. Images of the RCA were obtained with the transducer placed in the fourth and fifth intercostal spaces while the animals were in a left lateral recumbent position. When the transverse images of the aorta were identified in the left cranial parasternal short-axis view of the aorta, the right coronary cusp of the aorta was examined with 2D imaging and color flow mapping. Peak diastolic velocity and diastolic deceleration time of the RCAs and LCAs were measured by transthoracic pulsed-wave Doppler echocardiography with a sample volume of 1.5 mm and a frequency of 5.0 MHz.

All the data are expressed as the mean and standard deviation, and analyzed using statistical software (SPSS for Windows, ver. 19.0; SPSS, USA). An independent *t*-test with Bonferroni correction was used to compare the coronary artery diastolic peak velocities in each artery between the groups (control and MI dogs) and within each group (a p value < 0.01 was considered to be statistically significant). To evaluate the effect of observational variability on the measurement of diastolic peak velocity, two independent observers (Mr. Jaehwan Kim and Mr. Seungjun Lee) acquired images of coronary artery blood flow with pulsed wave Doppler echocardiography and recorded their results separately. Inter-observer agreement was assessed using two-way random intraclass coefficiency. Reproducibility was measured by conducting two transthoracic echocardiograph examinations 2 days apart for each dog. One-way intraclass coefficiency values were obtained to evaluate observed agreement. Inter- and intra-observer agreement was considered significant if the p value was less than 0.05.

Results

Before assessments of coronary arterial flow were made by transthoracic Doppler echocardiography, successful MI induction in all six MI dogs was confirmed by two-dimensional echocardiographic findings such as wall thinning, hyperechoic fibrosis, and hypokinesia of the infarcted segment of the left ventricular apex. However, other signs associated with MI, such as lethargy or exercise intolerance, were not observed in the MI group. After confirming MI induction by two-dimensional echocardiography, transthoracic echocardiographic evaluation of the coronary arteries was performed while the animals were conscious. To obtain images of the LCA, a clockwise-rotated beam angle (range: 28～47.7^{o}) in the right parasternal long-axis left ventricular outflow view was used. For the RCA, a clockwise-rotated inclined beam angle correction (range: 28～44^{o}) in the

left cranial parasternal short-axis view of the aorta was employed.

Hypoechoic coronary arteries were distinct from other cardiac structures on the two dimensional echocardiography images. The LCA was an infundibular structure arising from the sinus of Valsalva on the right parasternal long-axis left ventricular outflow view. The RCA appeared as tubular structures with the thin hyperechoic wall arising from the right coronary cusp of the aorta on the left cranial parasternal short-axis view. Blood flow of the LCA moved away from the probe on the color Doppler echocardiography whereas blood flowed toward the probe in the RCA. Systolic-(S) and diastolic-phase (D) waves for the RCA were found, but an S-wave was not observed in the LCA. Blood flow waves in the coronary arteries had rapid acceleration times and relatively long deceleration times (Fig. 2). The mean peak diastolic velocities of the LCAs and RCAs in the control group were 19.47 ± 2.67 and 20.84 ± 3.24 cm/sec, respectively (Table 1), and were not significantly different. Diastolic deceleration time of the LCA was slightly more rapid compared to that of the RCA (0.91 ± 0.14 sec *vs.* 1.13 ± 0.20 sec).

In the MI group, peak diastolic velocities and diastolic deceleration times of the LCAs and RCAs were significantly different from those of the control group (Fig. 2 and Table 1). Peak diastolic velocity of the LCA was significantly lower compared to that of the RCA in the MI group. Moreover, peak diastolic velocity of the LCA in the MI group was significantly slower relative to that of the control group (14.82 ± 1.61 cm/sec *vs.* 19.47 ± 2.67 cm/sec) and peak diastolic velocity of RCA in the MI group was significantly faster than that in the control group (31.61 ± 2.34 cm/sec *vs.* 20.84 ± 3.24 cm/sec; Table 1, Figs. 2 and 3). Diastolic deceleration time was also altered in the MI group. Diastolic deceleration time of the LCA was slightly slower in MI group compared with that in the control group (1.02 ± 0.22 sec *vs.* 0.91 ± 0.14 sec). The MI group had a significantly faster diastolic deceleration time in the RCA than the control group (0.71 ± 0.06 sec *vs.* 1.13 ± 0.20 sec). Differences in diastolic deceleration time between the LCA and RCA were significant and diastolic deceleration time of the LCA was slower than that of the RCA (1.02 ± 0.22 sec *vs.* 0.71 ± 0.06 sec; Table 1, Figs. 2 and 4).

There was strong agreement between the two individual observers who performed the coronary artery measurements. Reliability between the observers for the peak diastolic velocities of the LCA ($r = 0.70$, $p = 0.03$) and RCA ($r = 0.70$, $p = 0.03$) was significantly high for the control group. Reliability between observers for the peak diastolic velocities of the LCA ($r = 0.75$, $p = 0.03$) and

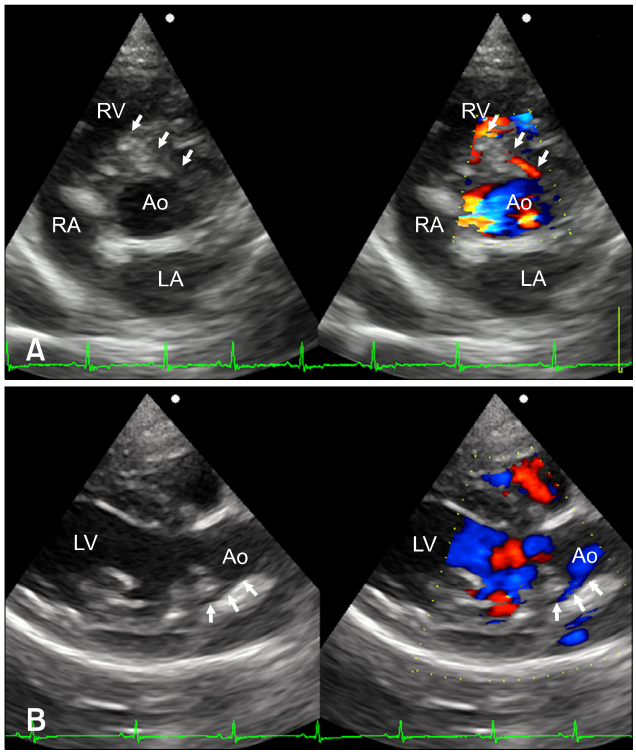

Fig. 1. Images of the coronary arteries with two-dimensional echocardiography (left) and color Doppler mapping (right). (A) Image of the right coronary artery (RCA; arrows) obtained from the modified left cranial short-axis view. (B) Image of the left coronary artery (LCA; arrows) acquired from the modified right parasternal long-axis left ventricular outflow tract view. RV: right ventricle, RA: right atrium, Ao: aorta, LA: left atrium, LV: left ventricle.

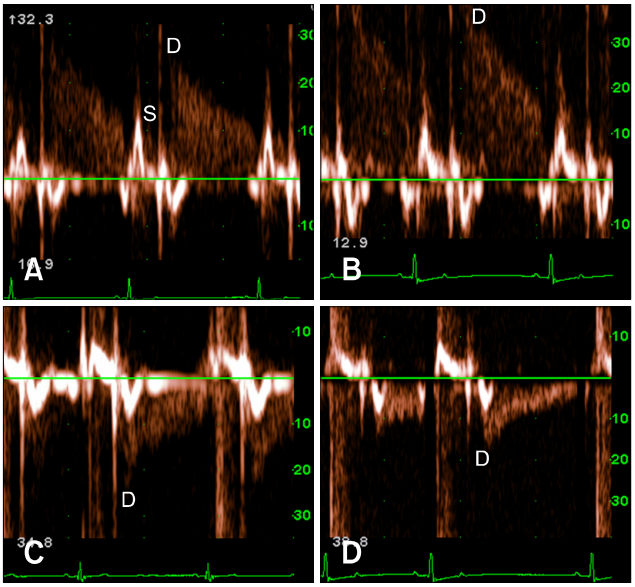

Fig. 2. Spectral Doppler mode images of coronary blood flow in the myocardial infarction (MI) group and control group. (A) RCA blood flow in a control dog. (B) RCA blood flow in a beagle with MI. (C) LCA blood flow in a control canine. (D) LCA blood flow in an animal with MI. S: systolic wave, D: diastolic wave.

RCA (r = 0.87, p = 0.01) in the MI group was also significantly high. For the diastolic deceleration time, reliability between observers of the LCA (r = 0.86, p = 0.02) and RCA (r = 0.94, $p < 0.01$) was indicative of good agreement in the control group. For the MI group, good inter-observer agreement for the diastolic deceleration times of the LCA (r = 0.94, $p < 0.01$) and RCA (r = 0.95, $p < 0.01$) was also observed.

Reproducibility had a trend similar to that of the inter-observer agreement. Reproducibility for the diastolic peak velocities of the LCA (r = 0.98, $p < 0.01$) and RCA (r = 0.85, $p < 0.01$) was significantly high in the control group. In the MI group, reproducibility for the diastolic peak velocities of the LCA (r = 0.91, $p < 0.01$) and RCA (r = 0.96, $p < 0.01$) was also significant. Reproducibility for the diastolic deceleration time of the LCA (r = 0.88, $p < 0.01$) and RCA (r = 0.93, $p < 0.01$) was observed in the control group. Significantly good agreement for diastolic deceleration time of the LCA (r = 0.93, $p < 0.01$) and RCA (r = 0.92, $p < 0.01$; Table 2) in the MI group was also found.

Table 1. Diastolic peak velocities and deceleration times in the coronary arteries of normal beagles and dogs with MI

	Control (n = 11)	MI (n = 6)
LCA peak D (cm/sec)	19.47 ± 2.67	14.82 ± 1.61*
RCA peak D (cm/sec)	20.84 ± 3.24	31.61 ± 2.34*,†
LCA DecT (sec)	0.91 ± 0.14	1.02 ± 0.22
RCA DecT (sec)	1.13 ± 0.20	0.71 ± 0.06*,†

*$p < 0.01$ *vs.* the control group; †$p < 0.01$ *vs.* the LCA. Control: normal dogs, MI: dogs with myocardial infarction, peak D: diastolic peak velocity, DecT: deceleration time.

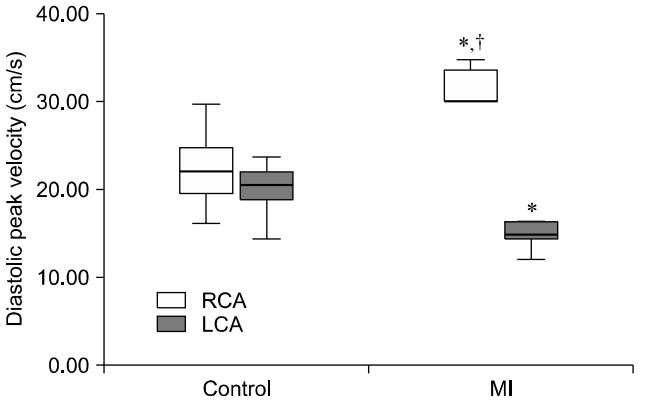

Fig. 3. Box-and-whisker plot of the diastolic peak velocity of normal dogs and model canines with MI. The MI group had significantly different peak diastolic velocities in the RCA and LCA compared to those for the control group (*). The RCA also had a more rapid peak diastolic velocity than that of the LCA in the MI group (†).

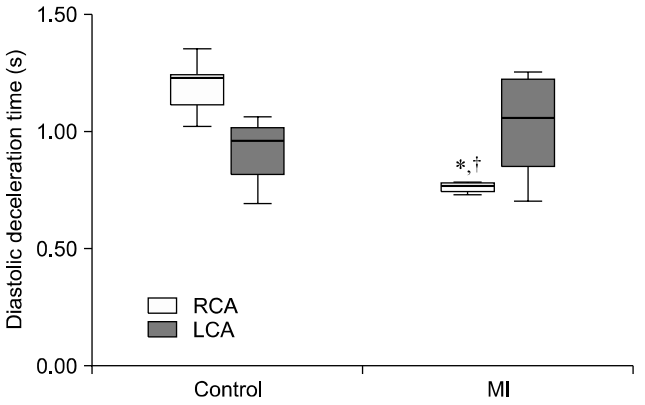

Fig. 4. Box-and-whisker plot of the diastolic deceleration time of normal dogs and model canines with MI. The RCA in the MI group had a rapid diastolic deceleration time compared to that of the RCA in the control group (*) and that of the LCA in the MI group (†).

Table 2. Inter- and intra-observer agreement for the coronary artery mean diastolic peak velocity and deceleration time

		Inter-observer agreement		Intra-observer agreement	
		r	p value	r	p value
Control (n = 11)	LCA peak D	0.70	0.03*	0.98	< 0.01*
	RCA peak D	0.70	0.03*	0.85	< 0.01*
	LCA DecT	0.86	0.02*	0.88	0.01*
	RCA DecT	0.94	< 0.01*	0.93	< 0.01*
MI (n = 6)	LCA peak D	0.75	0.03*	0.91	< 0.01*
	RCA peak D	0.87	0.01*	0.96	< 0.01*
	LCA DecT	0.94	< 0.01*	0.93	< 0.01*
	RCA DecT	0.95	< 0.01*	0.92	< 0.01*

*Agreement is significant ($p < 0.05$).

Discussion

For more accurate analyses of coronary artery blood profiles and hemodynamic measurements, it is preferable to use Doppler guidewire rather than transthoracic echocardiography given the low-quality images and limited frequency of transducers that are associated with the latter technique [34]. However, recent technological advances in digital imaging along with the introduction of high-frequency transducers have enabled the noninvasive and rapid evaluation of the coronary arteries by transthoracic echocardiography [34]. In the present study, we were able to monitor the canine coronary artery in high-resolution images obtained with color Doppler using high-frequency transducers. Echocardiographic coronary blood profiles were successfully acquired and normal coronary artery flow was easily differentiated from abnormal flow.

Images of the LCA obtained from the right parasternal long-axis left ventricular outflow view and short-axis view at the level of pulmonary artery showed that this artery arose from the left coronary cusp of the aorta. The right parasternal long-axis left ventricular outflow view allowed the coronary artery to be viewed more easily, and enabled the appropriate positioning of the beam angle along the line of blood flow for pulsed-wave Doppler analysis. The LCA was detectable when the transducer was rotated slightly clockwise in the right parasternal left ventricular outflow view to observe the left myocardium. This vessel was found to have an infundibular shape adjacent to the sinus of Valsalva and a thin hypoechoic tubular structure that split to form the paraconal branch. When the beam was inclined clockwise in the left cranial parasternal short-axis view of the aorta to observe the right myocardium, the RCA appeared as a thin tubular structure located at the 12 o'clock position relative to the aorta.

Blood flow velocity in the coronary artery measured using pulsed-wave Doppler analysis was similar to that described in previous studies using Doppler guidewire or intracardiac echocardiography [30]. Pulsed-wave Doppler analysis demonstrated the presence of S- and D-waves in the coronary artery. The S-wave of the systolic phase had a symmetrical waveform with a relatively short deceleration time and low peak velocity. The D-wave of the diastolic phase had a high acceleration time as well as a relatively slow and steady deceleration time and shoulder point. Deceleration times and peak velocities of the D- and S-waves were different.

In animals with cardiomyopathy [7,9,12,19,32], stenotic disease [4,11,14,23], myxomatous mitral valve disease [8,10,21,28,29], cardiovascular tumors [2], or dynamic changes in coronary flow may be associated with coronary arteriosclerosis and MI. A retrospective study on death caused by heart disease in Swedish dogs reported that 32 cases might be cardiomyopathy which was represented dilated cardiomyopathy or myocardial infarction secondary to arteriosclerosis of coronary artery or thromboembolism [9]. Previous studies demonstrated that feline cardiomyopathy presents as diffuse or segmental left ventricular hypertrophy that induces regional systolic dysfunction with myocardial fibrosis and matrix connective tissue accumulation accompanied by moderate or severe intramural coronary arteriosclerosis observed during necropsy [12,19]. In another study about feline hypertrophic cardiomyopathy, it was presumed that this coronary arterial condition could result in a reduction of coronary blood flow [7]. In cases of dilated cardiomyopathy, left ventricular fibrosis and intimal hyperplasia of the intramural coronary arteries also appear with thin and wavy myofibers in young Doberman pinschers with dilated myocardiopathy [32]. The thin and wavy myofibers are associated with changes of oxygen-dependent processes in myocytes as well as myocardial ischemia in humans and dogs [32]. Reverse systolic flow from the isometric ventricular contraction to the aortic ejection, concentric left ventricular hypertrophy, intramural thickening of the coronary arteries, and degeneration of left the ventricular myocardium have been found in dogs with subaortic stenosis [23]. Additionally, a relationship between intramural coronary atherosclerosis and left ventricular hypertrophy was reported in 49 dogs with subaortic stenosis, demonstrating that coronary atherosclerosis may be caused by excessive force generation secondary to left ventricular hypertrophy [11]. A case of left coronary aneurysmal dilation in a dog with subaortic stenosis was also described [14].

In the present study, the exact cause of LCA aneurysmal dilation was uncertain although elevated coronary vascular resistance secondary to left ventricular hypertrophy might have contributed to LCA dilation with poststenotic aortic outflow directed toward the LCA [14]. A previous study reported that English bulldogs with pulmonic stenosis showed congenital coronary artery anomaly of single RCA and abnormal circumpulmonary LCA [4]. Furthermore, myocardial infarction of the left ventricular wall was occurred in these dogs [4]. Causes of myocardial infarction in the left ventricle were not clarified in our investigation, but compression of the intramyocardial segment of the LCA is thought to be associated with hemodynamic changes at parturition [4]. In a previous study, proliferative changes and hyaline plaque formation were observed in dogs with myxomatous mitral valve disease [10]. These changes made the lumen of the coronary arteries narrower. Microscopic intramural MI is a common histopathologic finding in the heart of humans and canines with mitral valve disease [28]. Many factors promote intramural MI in dogs with mitral valve disease. Endothelial dysfunction of the coronary artery and microthrombosis due to platelet

aggregation are the most common factors. Previous studies on dogs with mitral valve disease showed that nitric oxide availability decreases in vessel endothelial cells with mitral regurgitation [8,21]. This results in vascular endothelial dilation impairment in the coronary artery, elevated vascular resistance, and intramural myocardial infarction secondary to insufficient oxygen delivery to the myocardium [8,21]. Platelet aggregation is commonly found in dogs with mitral regurgitant that also develop MI due to microthrombosis and perivascular fibrosis of the coronary artery which induces high vascular resistance [28,29]. Previously, a dog with aortic body carcinoma was reported with a mass located on the caudal left atrial epicardial surface that compressed the circumflex branch of the LCA [2]. The presence of MI was confirmed in the region that received blood from the circumflex branch of the LCA [2].

Changes in coronary blood flow are not only observed in cases of cardiovascular diseases such as hypertrophic cardiomyopathy [7,9,12,32] and mitral regurgitation [5,8,10,21,28,29], but also other pathologic conditions such as acute renal failure [18], chronic diabetes mellitus [13,15,31], and hypothyroidism [15,26]. In a previous study, dogs with acute renal failure had decreased or absent coronary flow reserve [18]. These coronary arterial flow changes were affected to dysfunction of coronary endothelium about vasodilation. The risk of myocardial infarction is increased if elevated oxygen demand of the myocardium is not satisfied by the coronary blood supply due to endotherial dysfunction of the coronary artery [18]. A previous study reported that 20 out of 30 dogs with diabetes mellitus or hypothyroidism developed atherosclerosis in the coronary artery [15]. Another investigation found that coronary blood flow in dogs with hypothyroidism was reduced compared to that in normal dogs [26]. Additionally, the coronary artery in cases of diabetes mellitus is not sufficiently dilated during exercise so coronary blood flow is less decreased [31] although this effect was not observe in subjects at rest [13].

In MI dogs with LCAs completely ligated below the first diagonal branch, blood flow in the RCA had a rapid diastolic deceleration time compared to the control animals. This was due to the supposed sympathetic reflex that is associated with MI and results in vascular constriction of the RCA, thereby increasing coronary pressure and flow [16,27]. The low diastolic peak velocity and slow deceleration time of blood flow in the LCA suggests that flow restriction is caused by total occlusion of the paraconal branch. Diastolic peak velocity differences between the control and MI groups were significant. This could have been due to collateral circulation from the paraconal branch and posterior descending artery [6]. In the MI group, blood flow velocity differences between the RCA and LCA were significant owing to higher RCA peak velocity values and lower LCA peak velocity values compared to those of normal dogs.

One limitation of this study is that we were unable to acquire images of the distal LCA or monitor S-waves. This was due to mitral inflow and myocardial interference. In addition, only beagles were used as a model of MI. For future studies, it would be beneficial to use animal models based on diverse species with different cardiovascular disease such as cats with hypertrophic cardiomyopathy.

In summary, transthoracic echocardiography enhanced coronary artery blood flow imaging with color Doppler. This helped detect differences in blood flow velocity and pulsed-wave Doppler patterns between dogs with MI and normal canines. Therefore, pulsed-wave Doppler examination of coronary arterial blood flow can be performed to evaluate hemodynamic function if echocardiographic equipment is available. In addition, application of this technique could be extended to evaluating myocardial blood flow in cases of other cardiovascular diseases.

Acknowledgments

This study was supported by Konkuk University in 2011.

References

1. **Akasaka T, Yoshida K, Hozumi T, Takagi T, Kaji S, Kawamoto T, Ueda Y, Okada Y, Morioka S, Yoshikawa J.** Restricted coronary flow reserve in patients with mitral regurgitation improves after mitral reconstructive surgery. J Am Coll Cardiol 1998, **32**, 1923-1930.
2. **Bossbaly MJ, Buchanan JW, Sammaro C.** Aortic body carcinoma and myocardial infarction in a dobermann pinscher. J Small Anim Pract 1993, **34**, 638-642.
3. **Botnar RM, Stuber M, Danias PG, Kissinger KV, Manning WJ.** Improved coronary artery definition with T2-weighted, free-breathing, three-dimensional coronary MRA. Circulation 1999, **99**, 3139-3148.
4. **Buchanan JW.** Pathogenesis of single right coronary artery and pulmonic stenosis in English bulldogs. J Vet Intern Med 2001, **15**, 101-104.
5. **Carabello BA, Nakano K, Ishihara K, Kanazawa S, Biederman RWW, Spann JF, Jr.** Coronary blood flow in dogs with contractile dysfunction due to experimental volume overload. Circulation 1991, **83**, 1063-1075.
6. **Chansky M, Levy MN.** Collateral circulation to myocardial regions supplied by anterior descending and right coronary arteries in the dog. Circ Res 1962, **11**, 414-417.
7. **Connolly DJ, Cannata J, Boswood A, Archer A, Groves EA, Neiger R.** Cardiac troponin I in cats with hypertrophic cardiomyopathy. J Feline Med Surg 2003, **5**, 209-216.
8. **Cunningham SM, Rush JE, Freeman LM.** Systemic inflammation and endothelial dysfunction in dogs with congestive heart failure. J Vet Intern Med 2012, **26**, 547-557.
9. **Egenvall A, Bonnett BN, Häggström J.** Heart disease as a

cause of death in insured Swedish dogs younger than 10 years of age. J Vet Intern Med 2006, **20**, 824-903.
10. **Falk T, Jönsson L, Olsen LH, Pedersen HD.** Arteriosclerotic changes in the myocardium, lung, and kidney in dogs with chronic congestive heart failure and myxomatous mitral valve disease. Cardiovasc Pathol 2006, **15**, 185-193.
11. **Falk T, Jönsson L, Pedersen HD.** Intramyocardial arterial narrowing in dogs with sub aortic stenosis. J Small Anim Prac 2004, **45**, 448-453.
12. **Fox PR.** Hypertrophic cardiomyopathy. Clinical and pathological correlates. J Vet Cardiol 2003, **5**, 39-45.
13. **Haider B, Ahmed SS, Moschos CB, Oldewurtel HA, Regan TJ.** Myocardial function and coronary blood flow response to acute ischemia in chronic canine diabetes. Circ Res 1977, **40**, 577-583.
14. **Hernandez JL, Bélanger MC, Benoit-Biancamano MO, Girard C, Pibarot P.** Left coronary aneurysmal dilation and subaortic stenosis in a dog. J Vet Cardiol 2008, **10**, 75-79.
15. **Hess RS, Kass PH, Van Winkle TJ.** Association between diabetes mellitus, hypothyroidism or hyperadrenocorticism, and atherosclerosis in dogs. J Vet Intern Med 2003, **17**, 489-494.
16. **Heusch G, Deussen A.** The effects of cardiac sympathetic nerve stimulation on perfusion of stenotic coronary arteries in the dog. Circ Res 1983, **53**, 8-15.
17. **Hozumi T, Yoshida K, Akasaka T, Asami Y, Ogata Y, Takagi T, Kaji S, Kawamoto T, Ueda Y, Morioka S.** Noninvasive assessment of coronary flow velocity and coronary flow velocity reserve in the left anterior descending coronary artery by Doppler echocardiography: comparison with invasive technique. J Am Coll Cardiol 1998, **32**, 1251-1259.
18. **Kingma JG, Jr., Vincent C, Rouleau JR, Kingma I.** Influence of acute renal failure on coronary vasoregulation in dogs. J Am Soc Nephrol 2006, **17**, 1316-1324.
19. **Kittleson MD, Meurs KM, Munro MJ, Kittleson JA, Liu SK, Pion PD, Towbin JA.** Familial hypertrophic cardiomyopathy in maine coon cats: an animal model of human disease. Circulation 1999, **99**, 3172-3180.
20. **Kurita T, Sakuma H, Onishi K, Ishida M, Kitagawa K, Yamanaka T, Tanigawa T, Kitamura T, Takeda K, Ito M.** Regional myocardial perfusion reserve determined using myocardial perfusion magnetic resonance imaging showed a direct correlation with coronary flow velocity reserve by Doppler flow wire. Eur Heart J 2009, **30**, 444-452.
21. **Moesgaard SG, Pederson LG, Teerlink T, Häggström J, Pederson HD.** Neurohormonal and circulatory effects of short-term treatment with enalapril and quinapril in dogs with asymptomatic mitral regurgitation. J Vet Intern Med 2005, **19**, 712-719.
22. **Pannu HK, Flohr TG, Corl FM, Fishman EK.** Current concepts in multi-detector row CT evaluation of the coronary arteries: principles, techniques, and anatomy. Radiographics 2003, **23** (Suppl 1), S111-S125.
23. **Pyle RL, Lowensohn HS, Khouri EM, Gregg DE, Patterson DF.** Left circumflex coronary artery hemodynamics in conscious dogs with congenital subaortic stenosis. Circ Res 1973, **33**, 34-38.
24. **Ropers D, Baum U, Pohle K, Anders K, Ulzheimer S, Ohnesorge B, Schlundt C, Bautz W, Daniel WG, Achenbach S.** Detection of coronary artery stenoses with thin-slice multi-detector row spiral computed tomography and multiplanar reconstruction. Circulation 2003, **107**, 664-666.
25. **Scheffel H, Stolzmann P, Plass A, Leschka S, Grünenfelder J, Falk V, Marincek B, Alkadhi H.** Coronary artery disease in patients with cardiac tumors: preoperative assessment by computed tomography coronary angiography. Interact Cardiovasc Thorac Surg 2010, **10**, 513-518.
26. **Scott JC, Balourdas TA, Croll MN.** The effect of experimental hypothyroidism on coronary blood flow and hemodynamic factors. Am J Cardiol 1961, **7**, 690-693.
27. **Shannon RP, Stambler BS, Komamura K, Ihara T, Vatner SF.** Cholinergic modulation of the coronary vasoconstriction induced by cocaine in conscious dogs. Circulation 1993, **87**, 939-949.
28. **Tanaka R, Murota A, Nagashima Y, Yamane Y.** Changes in Platelet life span in dogs with mitral valve regurgitation. J Vet Intern Med 2002, **16**, 446-451.
29. **Tarnow I, Kristensen AT, Olsen LH, Falk T, Haubro L, Pedersen LG, Pedersen HD.** Dogs with heart disease causing turbulent high-velocity blood flow have changes in platelet function and von Willebrand factor multimer distribution. J Vet Intern Med 2005, **19**, 515-522.
30. **Teragaki M, Toda I, Takagi M, Fukuda S, Ujino K, Takeuchi K, Yoshikawa J.** New applications of intracardiac echocardiography: assessment of coronary blood flow by colour and pulsed Doppler imaging in dogs. Heart 2002, **88**, 283-288.
31. **Tune JD, Yeh C, Setty S, Zong P, Downey HF.** Coronary blood flow control is impaired at rest and during exercise in conscious diabetic dogs. Basic Res Cardiol 2002, **97**, 248-257.
32. **Vollmar A, Fox PR, Meurs KM, Liu SK.** Dilated cardiomyopathy in juvenile Doberman pinschers. J Vet Cardiol 2003, **5**, 23-27.
33. **Yoshida K, Yoshikawa J, Hozumi T, Yamaura Y, Akasaka T, Fukaya T, Kato H.** Detection of left main coronary artery stenosis by transesophageal color Doppler and two-dimensional echocardiography. Circulation 1990, **81**, 1271-1276.
34. **Youn HJ, Foster E.** Demonstration of coronary artery flow using transthoracic Doppler echocardiography. J Am Soc Echocardiogr 2004, **17**, 178-185.